Influence of Interfacial Agents on the Physicochemical Characteristics of Binary Polyethylene/Polyamide 6 and Ternary Polyethylene/Polypropylene/Polyamide 6 Blends

PIER LUIGI BELTRAME,[1,]* ANTONELLA CASTELLI,[1] MARIO DI PASQUANTONIO,[1] MAURIZIO CANETTI,[2] and ALBERTO SEVES[2]

[1]Dipartimento di Chimica Fisica ed Elettrochimica, Università, I-20133 Milan, Italy; [2]Stazione Sperimentale per la Cellulosa, Carta e Fibre Tessili Vegetali e Artificiali, I-20133 Milan, Italy

SYNOPSIS

Binary low-density polyethylene/polyamide 6 and ternary low-density polyethylene/polypropylene/polyamide 6 blends were prepared by melt mixing, without and with the addition of two different commercial products [poly(ethylene-co-buthylacrylate-co-maleic anhydride) and poly(ethylene-co-vinylacetate) grafted with maleic anhydride] used as interfacial modifiers. More precisely, the polypropylene was a propylene/ethylene random copolymer, containing 6% by weight of ethylene. The polyamide 6/interfacial agent and polyethylene/interfacial agent systems were also considered. Differential scanning calorimetry, microscopic observations—together with chemical etchings—and mechanical tests supported the occurrence of strong interactions at the interface, especially when using the buthyl acrylate-based agent. The compatibilizing effect of the interfacial agents was also analyzed in the light of interfacial tension determinations. Eventually, low-density polyethylene modifications induced by compatibilization were studied carrying out WAXD analysis. © 1996 John Wiley & Sons, Inc.

INTRODUCTION

Most polymers are incompatible and their blending gives materials having poor interfacial adhesion and dispersion and poor mechanical properties with respect to the parent compounds. On the other hand, polymer blending could give a positive reply to the ever-growing industrial demand for new materials with a wide range of properties and a low cost/price ratio. Furthermore, blending could allow the recycling of plastic wastes and degraded polymeric materials.[1-13]

To improve the interfacial adhesion and the phase dispersion between immiscible polymers, which is a prerequisite for obtaining a compatibilization of their blends, an interfacial agent is usually added.[14-25] This should ensure a microscopic homogeneity, possibly combining some of the specific characteristics of blend components and gaining synergistic effects.
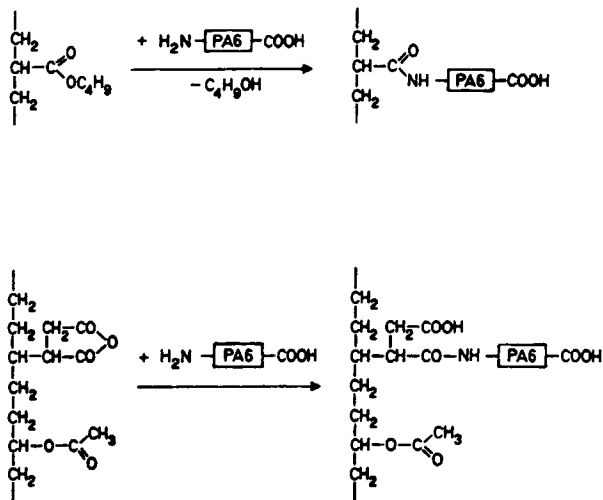
A typical example of immiscible polymers is the system consisting of polyolefins and polyamides, which are intrinsically different in terms of polarity. Blending of such polymers in the presence of proper compatibilizers could improve the impact resistance of the material as well as its resistance to oxygen permeation.

Several efforts have been devoted to compatibilize the blends of polyolefins and polyamides; in particular, functionalized polyolefins able to react with the amine end groups of polyamides have been considered as effective interfacial agents.[12,20-31] The chemical closeness, on one side, and the occurrence of chemical bonding, on the other, can ensure a tie between the different phases.

In this work, the effects of the addition of two commercial products, an ethylene/butylacrylate/maleic anhydride terpolymer and an ethylene/vinyl acetate copolymer modified with grafted maleic anhydride, were investigated in binary polyethylene/

---

polyamide 6 and ternary polyethylene/polypropyl-ene/polyamide 6 blends. It can be reasonably assumed that chemical bondings between butyl acrylate or maleic anhydride and terminal amine groups of polyamide 6 occur according to the following schemes:

$$
\begin{array}{c}
| \\
CH_2 \\
| \quad\quad O \\
CH-C \quad\quad + H_2N-\boxed{PA6}-COOH \\
| \quad OC_4H_9 \quad\quad \xrightarrow{-C_4H_9OH} \\
CH_2 \\
|
\end{array}
\quad
\begin{array}{c}
| \\
CH_2 \\
| \quad\quad O \\
CH-C \\
| \quad\quad NH-\boxed{PA6}-COOH \\
CH_2 \\
|
\end{array}
$$

$$
\begin{array}{c}
| \\
CH_2 \\
| \quad CH_2-CO \\
CH_2 \quad\quad\quad O \\
CH-CH-CO \\
| \\
CH_2 \\
| \\
CH_2 \\
| \quad\quad CH_3 \\
CH-O-C \\
| \quad\quad\quad O \\
CH_2 \\
|
\end{array}
\quad + H_2N-\boxed{PA6}-COOH \longrightarrow
\quad
\begin{array}{c}
| \\
CH_2 \\
| \quad CH_2-COOH \\
CH_2 \\
CH-CH-CO-NH-\boxed{PA6}-COOH \\
| \\
CH_2 \\
| \\
CH_2 \\
| \quad\quad CH_3 \\
CH-O-C \\
| \quad\quad\quad O \\
CH_2 \\
|
\end{array}
$$

This allows the blend components to disperse each other and the copolymers to act as compatibilizing agents.

Differential scanning calorimetry and microscopic observations performed on the polymeric systems before and after chemical etchings supported the presence of a strong interfacial interaction in polyolefin/polyamide blends promoted by the compatibilizing agents. This was confirmed by some mechanical tests. The effectiveness of the compatibilization has been also examined in the light of the interfacial tension variations associated with the addition of the interfacial agents. Eventually, the polyethylene structural changes in the binary blends have been determined by wide-angle X-ray diffraction measurements.

EXPERIMENTAL

Materials

The polymers used in this work were a low-density polyethylene (LDPE), manufactured by Enichem (Riblene FM34), a polypropylene–ethylene random copolymer containing 6% by weight of ethylene (PP), manufactured by Petrochemie Danubia (Daplen KFC 2006), a polycaprolactam (PA6), manufactured by EMS Chemie (Grilon F34), and, as possible compatibilizing agents, an ethylene/butylacrylate/maleic anhydride (91/8/1, by weight)

terpolymer (LO), manufactured by ELF Atochem (Lotader 3210), and an ethylene/vinylacetate copolymer (91/9, by weight) modified with 1% by weight of grafted maleic anhydride (EV), manufactured by Enichem (Evagam Primeflex AL34L).

Development of the Blends

All the blends were prepared in the form of 20 mm-wide and 0.5 mm-thick strips by melt mixing in a Gimac single-screw microextruder, keeping the temperature of the three zones at 230, 235, and 235°C and the die temperature at 230°C. The screw speed was kept at 25–30 rpm. Before mixing in a one-step process, the components were separately ground and sieved (20 mesh) and PA6 was dried for 105 min at 105°C.

Binary blends were extruded with LDPE/PA6 weight ratios 100/0, 70/30, 50/50, 30/70, and 0/100. When a compatibilizing agent (c.a.) was employed, 2.5–10 parts of it were added to 100 parts of the blends.

Ternary blends were extruded with LDPE/PP/PA6 weight ratios 35/35/30. When a compatibilizer was employed, 5 parts of it were added to 100 parts of the blend. LDPE/c.a. and PA6/c.a. systems were also extruded, using the same conditions as above.

Thermal Determinations

In the study of the thermal behavior of the blends, a differential scanning calorimeter (Perkin-Elmer DSC-4) was used, operating at the following conditions: the specimens (8–10 mg), encapsulated in aluminum pans, were rapidly heated to 260°C, held 30 min at this temperature in order to cancel their thermal history, cooled to 0°C at a scanning rate of 20°C/min, and eventually heated again to 260°C at the same rate. The thermal behavior of the compatibilized blends was compared with the corresponding data for the polymer blends without the compatibilizer. All the experiments were performed under a constant flow of dry nitrogen. An indium standard sample was employed to determine the thermal lag due to the scanning rate and to calibrate the heat of transition.

Structural and Morphological Determinations

Wide-angle X-ray Diffraction (WAXD)

The measurements were carried out on the extruded materials at 20°C using a Siemens D-500 diffractometer. Monochromatized CuKα radiation (λ

= 1.541 Å) with a nickel filter was generated by a Siemens Kristalloflex 810 generator. The operating voltage and current were 45 kV and 25 mA. The samples were mounted on a carrier for specimen spinning with a rotational speed of 30 rpm. The data were collected (0.02 2θ intervals) and treated by the Diffrac-AT V 3.2 software controlling the system. The degree of crystallinity was calculated from diffracted intensity data in the range $2\theta = 10°-30°$ by using the area integration method. The apparent crystal size of the plain and blended LDPE was calculated from the line-broadening data by the Scherrer equation[32] in the direction perpendicular to the (110) crystallographic plane. A nickel standard sample was employed to determine the instrumental broadening.

Scanning Electron Microscopy (SEM)

The samples, fractured under liquid nitrogen, were observed with a scanning electron microscope, Philips Model 55, operated at 9.4–9.9 kV. The surfaces of the fractured specimens were coated with gold.

Mechanical Determinations

An Instron machine Model 1122 operating at 23°C and 50% RH was used for tensile properties measurements (MA). The crosshead speed was kept at 50 mm/min and the gauge length was 50 mm in all the determinations. The specimens for the tensile tests were cut out from the extruded strips and equilibrated under ambient conditions (23°C and 50% RH) for at least 24 h. The reported data are the results of an average of 10–12 measurements.

Treatment of Polymers with Formic Acid

PA6-containing materials were treated with formic acid to remove the polyamide fraction not bound to the compatibilizer in order to properly characterize the remaining residual compound. The PA6/c.a. material was finely cut, immersed in 88% formic acid, vigorously and repeatedly shaken, and then left standing in the solution during 48 h; afterward, the resulting suspension was centrifuged and the upper turbid layer collected and repeatedly washed with fresh acid solution. This product was subjected to thermal and elemental analyses. For the morphological analysis, the polyolefin/polyamide blend strips were cut or fractured, treated with 88% formic acid solutions for 48 h, and dried in a pistol at 65°C overnight and the sections observed with the scanning electron microscope.

Contact Angle and Surface Tension Measurements

The contact angle measurements were carried out to determine the surface tensions of the polymers and the interfacial tensions between them. The drop bubble method[33] was used operating at 23°C and 50% RH with a Lorentzen and Wettres machine. As the two phases representative of strong dispersion and polar effects, methylene iodide (MI) and water (W) were chosen. For the indirect determination of the surface tension of the polymers, the following dispersion and polar components of the surface tension of MI and W were employed: $\gamma^d_{MI} = 44.1$; $\gamma^p_{MI} = 6.7$; $\gamma^d_W = 22.1$; $\gamma^p_W = 50.7$ dynes/cm.[33,34] The surface tension of a given polymer P (single polymer or polymer + interfacial agent) was evaluated by adding the corresponding dispersion and polar components: $\gamma_P = \gamma^d_P + \gamma^p_P$.[35,36] These components were obtained by solving the following system[35]:

$$
\begin{cases}
(\gamma^d_{MI} + \gamma^p_{MI} - \alpha_{MI})\gamma^d_P\gamma^p_P + \gamma^d_{MI}(\gamma^p_{MI} - \alpha_{MI})\gamma^p_P \\
\quad + \gamma^p_{MI}(\gamma^d_{MI} - \alpha_{MI})\gamma^d_P - \alpha_{MI}\gamma^d_{MI}\gamma^p_{MI} = 0 \\
(\gamma^d_W + \gamma^p_W - \alpha_W)\gamma^d_P\gamma^p_P + \gamma^d_W(\gamma^p_W - \alpha_W)\gamma^p_P \\
\quad + \gamma^p_{MI}(\gamma^d_W - \alpha_W)\gamma^d_P - \alpha_W\gamma^d_W\gamma^p_W = 0 \quad (1)-(2)
\end{cases}
$$

The first equation of the system refers to measurements of the contact angle $\theta_{MI/P}$ between MI and P, being[35]

$$
\alpha_{MI} = \tfrac{1}{4}(\gamma^d_{MI} + \gamma^p_{MI})(1 + \cos\theta_{MI/P})
$$

$$
= \tfrac{1}{4}\gamma_{MI}(1 + \cos\theta_{MI/P}) \quad (3)
$$

The second equation refers to measurements of contact angle $\theta_{W/P}$ between W and P, being[35]

$$
\alpha_W = \tfrac{1}{4}(\gamma^d_W + \gamma^p_W)(1 + \cos\theta_{W/P})
$$

$$
= \tfrac{1}{4}\gamma_W(1 + \cos\theta_{W/P}) \quad (4)
$$

RESULTS AND DISCUSSION

The binary LDPE/PA6 blends, cooled from the melt in DSC, showed two exothermic peaks due to the PA6 and LDPE crystallization, respectively. The same blends showed two endothermic peaks of melting, as they were heated up to 260°C.

The behavior of PA6 in these blends, prepared with different weight ratios of the components, in the absence of LO or EV and with different amounts

Table I   Degrees of Crystallinity (x_c, x_m) of PA6 in LDPE/PA6 Blends, Obtained from the Enthalpies of Crystallization and of Melting in DSC, in the Presence of Different Amounts of c.a. ($\Delta H^0_{m,PA6} = 55.0$ cal/g)[a]

LDPE/PA6/c.a.	LO		EV	
	x_c	x_m	x_c	x_m
0/100/0	0.27	0.26	0.27	0.26
70/30/0	0.26	0.26	0.26	0.26
70/30/2.5[b]	0.13	0.23	0.17	0.22
70/30/5	0.13	0.22	0.16	0.23
70/30/10	0.02	0.24	0.21	0.23
50/50/0	0.29	0.28	0.29	0.28
50/50/4.17[b]	0.23	0.25	0.23	0.26
30/70/0	0.28	0.28	0.28	0.28
30/70/5.83[b]	0.25	0.25	0.26	0.27

[a] Ref. 34.
[b] PA6/c.a. weight ratio = 30/2.5.

Table II   Degrees of Crystallinity (x_c, x_m) of PA6 in PA6/c.a. Systems, Obtained from the Enthalpies of Crystallization and of Melting in DSC ($\Delta H^0_{m,PA6} = 55.0$ cal/g)[a]

PA6/c.a.	LO		EV	
	x_c	x_m	x_c	x_m
30/0	0.27	0.26	0.27	0.26
30/2.5	0.27	0.27	0.28	0.28
30/5	0.24	0.24	0.26	0.25
30/10	0.24	0.24	0.26	0.27[b]

[a] Ref. 34.

of them added to 100 parts of the blend, is shown in Table I, in which x_c is the degree of crystallinity calculated from the enthalpies of crystallization, while x_m is the degree of crystallinity calculated from the enthalpies of melting.

Taking into account the 70/30 LDPE/PA6 ratio, one observes that the values of x_c markedly decreases with the increase of the interfacial agent amount, apart one case (EV, 10 parts added to 100 parts of 70/30 LDPE/PA6 blend). This exception will be also observed in the mechanical tests. It must be noticed that the relatively high cooling rate employed in DSC (20°C/min) and the amount of LDPE present in the blend emphasized the interaction phenomena due to the interfacial agents during PA6 crystallization. x_m values demonstrate that PA6 could crystallize to a greater extent than that shown by x_c data, although no other exothermic peak occurred either in the cooling or in the heating scans, except the LDPE one.

When the PA6 content in the plain blends was increased, the crystallization data remained substantially unchanged, while some variations were observed in the presence of LO as well as of EV. However, the lowering of x_c values in blends having a constant 30/2.5 PA6/c.a. weight ratio was marked in LDPE-rich blends, while this was not equally evident in PA6-rich ones. The importance of the presence of LDPE on the PA6/c.a. interaction extent can particularly be inferred from the data in Table II. For instance, considering the 70/30/10 LDPE/PA6/LO blend (Table I) and the 30/10 PA6/LO system (Table II), an x_c value of 0.02 is observed in

the former case vs. a value as high as 0.24 in the latter. On the basis of the x_c data in Table I, LO appears to be the more disturbing agent in the PA6 crystallization, thus evidencing its higher effectiveness in compatibilizing LDPE/PA6 blends.

Examples of the calorimetric scans of the considered blends are drawn in Figure 1. This shows the crystallization peaks of LDPE and PA6 in 70/30 LDPE/PA6 blends in the presence of different amounts of the compatibilizer. With LO as well as with EV, the exothermic peak of PA6 (the small one
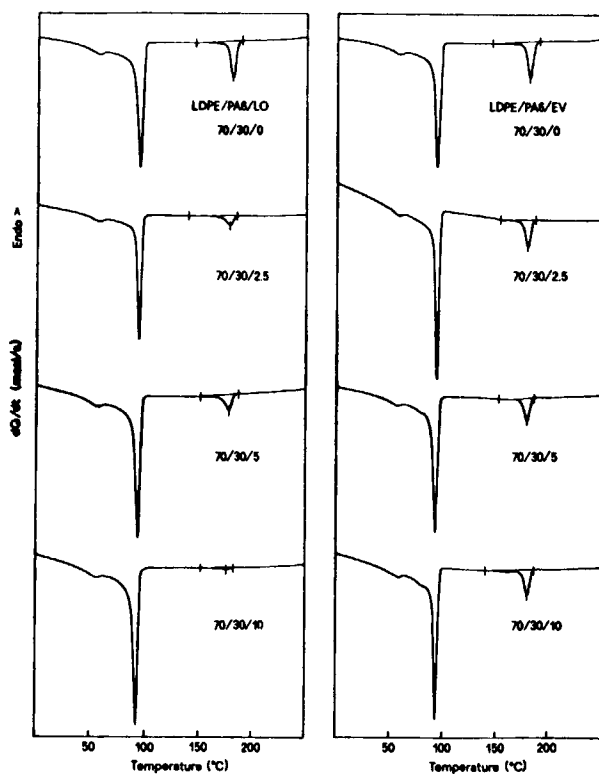

Figure 1   DSC cooling scans of LDPE/PA6/c.a. blends at different weight ratios.

Table III   PA6/c.a. Weight Ratios[a] Before and After Washing with Formic Acid

PA6/c.a. Before Washing	PA6/LO After Washing	PA6/EV After Washing
30/2.5	0.12	0.052
30/5	0.20	0.053
30/10	0.52	0.075

[a] From nitrogen elemental analysis.

on the right) progressively decreases with the increase of the quantity of the interfacial agent (apart the aforementioned exception), mainly in the case of LO.

To isolate the interactions between PA6 and the compatibilizing agents, PA6/c.a. systems were etched with formic acid to remove the unbound fraction. Washing with formic acid did not completely dissolve PA6; in the case of the 30/10 PA6/LO system, it remained associated with LO in a $\frac{1}{2}$ weight ratio (from nitrogen elemental analysis). It was found that such a ratio lowers with the decrease of the LO amount in the system as shown in Table III. Data in the same table indicate that the amount of PA6 involved in the chemical bonding with EV is quite smaller than with LO.

Tables IV and V report the crystallization and melting temperatures of the components of PA6/c.a. system at various weight ratios before and after the chemical etching. Inspection of these tables reveals that, after washing, temperatures T_c of PA6

and the compatibilizing agent approach each other and so do temperatures T_m, thus confirming the existence of a strong interaction between the two polymers. Again, LO functions to a greater extent than does EV. An example of such an approach is shown in Figure 2.

The degrees of crystallinity (x_c, x_m) of LDPE in binary LDPE/PA6 blends, obtained from the calorimetric data, are collected in Table VI. Also, in this case, the degree of crystallinity decreases in the presence of the compatibilizing agent with respect to the plain blend, as will be further discussed when examining WAXD data. However, the nature of the polyolefin/c.a. interaction is intrinsically different from that of PA6/c.a., since neither chemical bondings nor polar interactions can play a role.

Finally, the thermal behavior of PA6 in ternary LDPE/PP/PA6 blends is summarized in Table VII. Considerations analogous to those relative to Table I can be made, the data being quite analogous to those of LDPE/PA6/LO 70/30/5 blends. The influence of LO on PA6 crystallization confirms to be stronger than that of EV.

The compatibilization power of the two considered interfacial agents and the different extent to which they work in the two cases was visualized carrying out a morphological analysis on the cryogenic fractured surfaces of the blend strips by scanning electron microscopy (Fig. 3). In the incompatible binary blend [Fig. 3(a)], there are large domains of PA6 resembling carrots having a diameter of about 10 μm. By contrast, in the compatibilized

Table IV   Crystallization Temperature (T_c) from DSC Analysis of the Components of PA6/c.a. System at Various Weight Ratios Before and After Washing with Formic Acid

Sample	$T_{c_{PA6}}$ (°C)		$T_{c_{c.a.}}$ (°C)	
	Before Washing	After Washing	Before Washing	After Washing
PA6/LO				
30/0	179.4	—	—	—
0/30	—	—	81.3	81.3
30/2.5	179.1	—	82.3	87.4
30/5	176.9	162.7	83.5	87.3
30/10	173.8	166.9	82.9	87.3
PA6/EV				
30/0	179.4	—	—	—
0/30	—	—	77.5	77.5
30/2.5	180.1	179.2	79.7	81.8
30/5	179.9	—	79.6	81.4
30/10	179.0	—	79.5	81.2

Table V   Melting Temperatures (T_m) from DSC Analyses of the Components of PA6/c.a. System at Various Weight Ratios Before and After Washing with Formic Acid

Composition	$T_{m_{PA6}}$ (°C)		$T_{m_{LO}}$ (°C)	
	Before Washing	After Washing	Before Washing	After Washing
PA6/LO				
30/0	219.9	—	—	—
0/30	—	—	103.2	103.2
30/2.5	219.0	215.6	100.8	105.9
30/5	220.8	215.7	103.1	104.2
30/10	218.3	215.8	101.7	104.8
PA6/EV				
30/0	219.9	—	—	—
0/30	—	—	98.6	98.6
30/2.5	218.6	215.0	95.4	98.0
30/5	220.7	212.7	97.3	98.7
30/10	219.2	215.1	96.4	99.1

blends, PA6 is hardly distinguishable from LDPE [Fig. 3(b) and (c)]. It can be observed that the best dispersion occurred in the presence of LO. This was confirmed by SEM analyses carried out on the etched sections of uncompatibilized and differently compatibilized blends. An example is reported in Figure 4: In the case of the plain blend, large holes can be seen corresponding to the PA6 removed by formic acid, while in the presence of LO, the surface morphology suggests a markedly improved fine dispersion of the polyamidic phase. On the other hand, the effect of adding EV appears to be rather scarce. The SEM micrographs of ternary LDPE/PP/PA6 blends are collected in Figure 5, the inspection of

which reveals morphological effects analogous to the ones described above.

The mechanical properties at yield and the values of the Young's modulus of single polymers LDPE, PP, and PA6 and of their binary and ternary blends, without and with different amounts of the compatibilizing agent, are collected in Table VIII. In the case of 70/30 LDPE/PA6 blends, an improvement of properties is induced by the presence of LO as well as of EV; for the more effective compatibilizer,
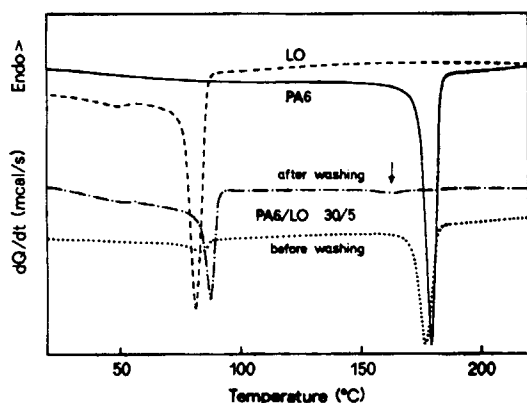

Figure 2 DSC cooling scans of the PA6/LO 30/5 system, before and after washing with formic acid, and scans of the pure polymers.

Table VI   Degrees of Crystallinity (x_c, x_m) of LDPE in LDPE/PA6 Blends, Obtained from the Enthalpies of Crystallization and of Melting in DSC, in the Presence of Different Amounts of c.a. ($\Delta H^0_{m,LDPE}$ = 70.2 cal/g)[a]

LDPE/PA6/c.a.	LO		EV	
	x_c	x_m	x_c	x_m
100/0/0	0.44	0.46	0.44	0.46
70/0/5	0.41	0.40	0.41	0.39
70/30/0	0.42	0.43	0.42	0.43
70/30/2.5[b]	0.37	0.40	0.38	0.39
70/30/5	0.39	0.39	0.40	0.39
70/30/10	0.36	0.37	0.36	0.37
50/50/0	0.41	0.42	0.41	0.42
50/50/4.17[b]	0.39	0.38	0.33	0.36
30/70/0	0.41	0.41	0.41	0.41
30/70/5.83[b]	0.32	0.32	0.30	0.31

[a] Ref. 34.
[b] PA6/c.a. weight ratio = 30/2.5.

Table VII Degrees of Crystallinity (x_c, x_m) of PA6 in Ternary LDPE/PP/PA6 Blends, Without or With c.a.

LDPE/PP/PA6/c.a.	x_c	x_m
0/0/100/0	0.27	0.26
35/35/30/0	0.28	0.26
35/35/30/5 (LO)	0.14	0.22
35/35/30/5 (EV)	0.21	0.24

LO, on going from 0 to 10 parts of LO added to 100 parts of 70/30 LDPE/PA6, strain and stress parameters regularly increase, progressively approaching values rather close to those expected on the basis of additive rules. Considering the binary blends with a constant PA6/c.a. weight ratio, it can be seen that the amount of LDPE plays an important role in improving their tensile properties when compared to those of the uncompatibilized mixture. The above considerations qualitatively hold also when using EV, apart the anomalous behavior of 70/30/10 LDPE/PA6/EV blend that can be noted as well in DSC measurements (see x_c values in Table I). The higher improvement of tensile properties in the ternary blend is again achieved by using LO, as shown also by data in Table IX, which collects the mechanical parameters at break.

Since the interfacial agent essentially works interacting with the components of the blend, PA6/c.a. systems were considered. Trends of the Young's modulus and stress at yield vs. composition are depicted in Figure 6. The close connection of the components PA6 and LO can be inferred from the values of the mechanical parameters of the PA6/LO system that are intermediate between those of the pure

polymers. Conversely, in PA6/EV blends, the mechanical behavior resembles that of EV.

The compatibilization efficiency was also investigated in the light of the interfacial tension lowering due to the presence of interfacial agents. The closer to zero the value of the interfacial tension in the compatibilized blend, the more effective is the compatibilization.

The interfacial tension between two polymers P1 and P2 ($\gamma_{P1//P2}$, in the incompatible system) was calculated by using the harmonic mean equation[37]:

$$\gamma_{P1//P2} = \gamma_{P1} + \gamma_{P2} - \frac{4\gamma_{P1}^d \gamma_{P2}^d}{\gamma_{P1}^d + \gamma_{P2}^d} - \frac{4\gamma_{P1}^p \gamma_{P2}^p}{\gamma_{P1}^p + \gamma_{P2}^p} \quad (5)$$

where γ_{P1} and γ_{P2} are the surface tension of the pure components, γ^d and γ^p being their dispersion and polar components ($\gamma = \gamma^d + \gamma^p$).[33,35,37,38] The interfacial tension between two parent compounds, both modified with LO or EV ($\gamma_{P1'//P2'}$, in the compatibilized system) was calculated in a way analogous to the one described above.

The dispersion and polar components of the surface tension were determined as described in the Experimental section. The contact angles and the surface tensions with their dispersion and polar components relative to all the various systems considered are reported in Table X. As expected, the γ^p values of functionalized polyolefins (LO and EV) are clearly higher than those of LDPE and PP. The strong polarity of EV is reasonably due to the greater polarity of its vinyl acetate unit with respect to the butyl acrylate one, proper of LO.

The comparison of the interfacial tension between pure LDPE and PA6 with those between the same polymers modified by adding LO or EV (see
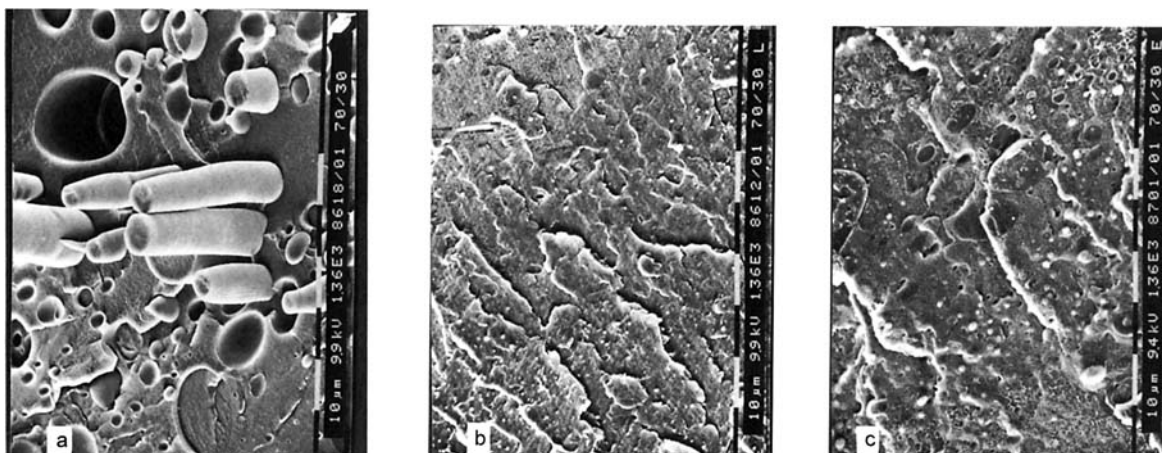

Figure 3 SEM micrographs of binary blends: (a) LDPE/PA6 70/30; (b) LDPE/PA6/ LO 70/30/5; (c) LDPE/PA6/EV 70/30/5.
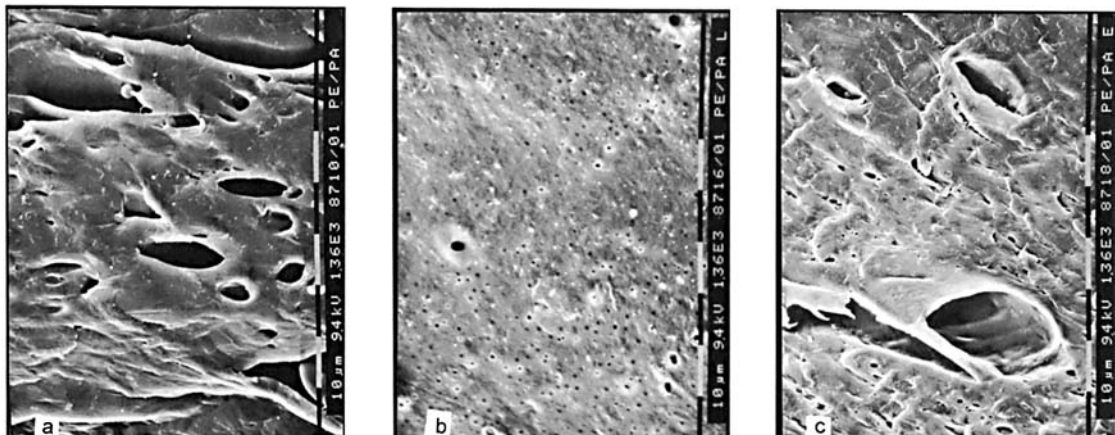
Figure 4 SEM micrographs of binary blends after chemical etching with formic acid:
(a) LDPE/PA6 70/30; (b) LDPE/PA6/LO 70/30/5; (c) LDPE/PA6/EV 70/30/5.

Table XI) shows a drop of the $\gamma_{P1//P2}$ value in the former case and a moderate, even if significant, decrease in the latter: this suggests that an enhanced adhesion of the polyolefinic and polyamidic phases can occur. However, it must be taken into account that in polymer mixtures the lower surface energy compound probably concentrates on the surface,[33,39,40] so that contact angle measurements of PA6/c.a. systems could be affected by this factor. In other words, the surface of the PA6/c.a. materials could resemble that of the compatibilizing agent or, even, it could have an energy which is lower than those of both PA6 and the compatibilizer, because of an increased packing of polar groups in the material and of the submergence of the hydrocarbon chains on the surface.[39]

Inspection of Table XII, which collects the interfacial tensions of all the possible polymer pairs, indicates that LDPE and PP combined together present a $\gamma_{P1//P2}$ value close to zero, while high $\gamma_{P1//P2}$ values are obtained when each of them is combined with PA6. Furthermore, it can be observed that the interfacial tension of the LDPE//LO pair is lower than that of the LDPE//EV pair and that the one of PA6//LO is higher than that of PA6//EV. The first result justifies the greater compatibilization power of LO on the polyolefinic side, while the second does not on the polyamidic side. Evidently, another factor is to be at work: Reasonably, LO has more possibilities than does EV to give chemical bondings with its numerous anhydride and ester reactive groups (see also Table III).

The reduction in the crystallization extent of LDPE observed by DSC measurements on the considered blends, due to the compatibilization involving an extended dispersion of phases, was also evidenced by carrying out WAXD measurements. The crystallization degree (x), the apparent crystal size
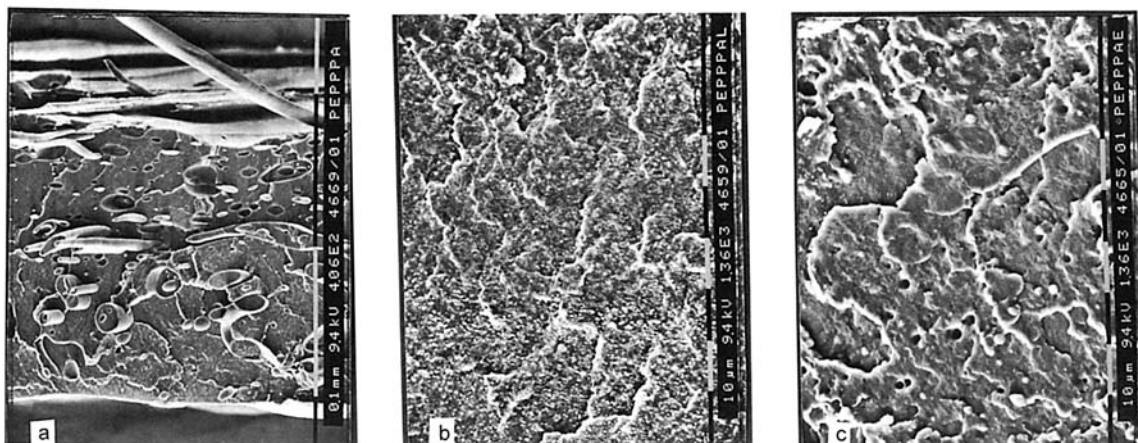

Figure 5 SEM micrographs of ternary blends: (a) LDPE/PP/PA6 35/35/30; (b) LDPE/PP/PA6/LO 35/35/30/5; (c) LDPE/PP/PA6/EV 35/35/30/5.

Table VIII Tensile Mechanical Properties at Yield of Blends Containing LDPE, PP, PA6, and c.a. at Different Weight Ratios, Tested with a Crosshead Speed of 50 mm/min at 23°C

	LO			EV		
LDPE/PP/PA6/c.a.	Strain at Yield (%)	Stress at Yield (kg/mm²)	Young's Modulus (kg/mm²)	Strain at Yield (%)	Stress at Yield (kg/mm²)	Young's Modulus (kg/mm²)
100/0/0/0	77.4	0.87	13.1	77.4	0.87	13.1
0/100/0/0	12.8	2.37	62.5	12.8	2.37	62.5
0/0/100/0	21.8	3.69	56.6	21.8	3.69	56.6
70/0/30/0	13.3	1.09	22.9	13.3	1.09	22.9
70/0/30/2.5[a]	36.0	1.23	20.5	19.0	1.21	21.7
70/0/30/5	42.8	1.51	18.7	41.1	1.15	15.2
70/0/30/10	56.1	1.71	19.0	34.1	1.22	20.0
50/0/50/0	23.3	1.65	30.0	23.3	1.65	30.0
50/0/50/4.17[a]	25.1	1.55	27.4	23.3	1.72	24.8
30/0/70/0	19.0	2.02	33.8	19.0	2.02	33.8
30/0/70/5.83[a]	28.8	2.05	32.7	—	—	30.8
50/50/0/0	19.5	1.55	36.2	19.5	1.55	36.2
35/35/30/0	11.4	1.55	40.4	11.4	1.55	40.4
35/35/30/5	20.4	1.79	37.9	18.3	1.73	34.7

[a] PA6/c.a. weight ratio = 30/2.5.

in the direction perpendicular to the (110) crystallographic plane (D_{110}), the cell parameters (a, b, and c), and the consequent specific volume (v) are reported in Table XIII, where LDPE/PA6 blends are considered without and with different amounts of LO. The specific volume values were calculated according to the following equation:

$$v = \frac{a \times b \times c \times 10^{-24}}{2 \times 46.564 \times 10^{-24}} \frac{cm^3}{g} \qquad (6)$$

For the 30/70 LDPE/PA6 blends, the extended broadening of the peak relative to the (011) plane allowed no reliable evaluations of the c-cell parameter.

Table IX Tensile Mechanical Properties at Break of Ternary LDPE/PP/PA6 Blends, Tested with a Crosshead Speed of 50 mm/min at 23°C

LDPE/PP/PA6/c.a.	Strain at Break (%)	Stress at Break (kg/mm²)
35/35/30/0	27.9	0.57
35/35/30/5 (LO)	371.1	2.01
35/35/30/5 (EV)	139.2	1.15

As expected, the crystallization degree of LDPE decreases in the presence of LO and, to a greater extent, with the decrease of LDPE/PA6 ratio; correspondingly, there is an increase of specific volume values. These results can be reasonably explained
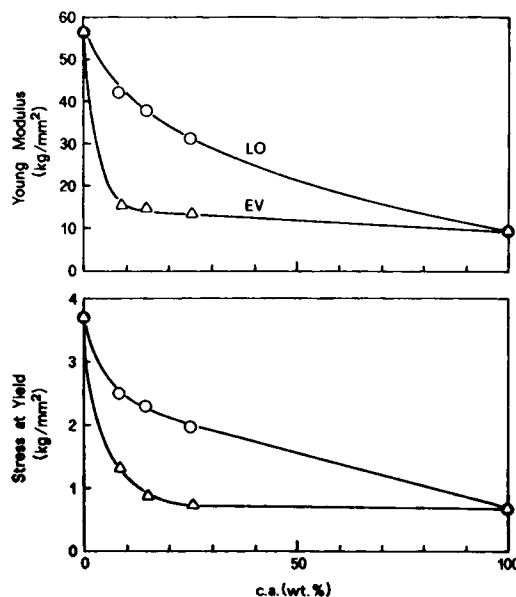

Figure 6 Trends of tensile mechanical properties vs. composition in PA6/c.a. systems.

Table X   Measurements of Contact Angles Between Methylene Iodide (θ_{MI}) or Water (θ_W) and Polymer Systems and Resulting Polymer System Surface Tension Data

	θ_{MI} (°)	θ_W (°)	γ^d (dynes/cm)	γ^p (dynes/cm)	γ (dynes/cm)
LO	52.2	92.3	29.0	5.5	34.5
EV	51.3	81.8	26.5	10.6	37.1
LDPE	56.1	97.3	28.9	3.6	32.5
LDPE/LO 70/5	53.2	92.1	28.2	5.7	33.9
LDPE/EV 70/5	51.7	82.6	26.4	10.2	36.6
PP	61.1	101.0	27.6	2.6	30.2
PA6	41.8	69.1	28.9	16.0	44.9
PA6/LO 30/5	54.5	94.8	28.6	4.6	33.2
PA6/EV 30/5	52.9	95.6	30.0	4.0	34.0

considering that LDPE finds it difficult to arrange in the crystalline cell all the different kinds of imperfections consisting of the polar and bulky groups present in the LO polymer chain and, especially, considering that its crystallization is inhibited, being finely dispersed with PA6 by the action of LO.

The apparent crystal size of LDPE in the direction perpendicular to the (110) crystallographic plane was calculated by using the Scherrer equation:

$$D_{hkl} = \frac{K \times \lambda}{\beta_0 \times \cos(\Theta_{hkl})} \tag{7}$$

where β_0 is the half-width in radiants of the reflections corrected for instrumental broadening, and λ, the wavelength of the X-ray radiation employed. The shape factor K was set equal to unity, and, thus, the size data have to be considered as relative data.[32] The D_{110} values in Table XIII show significant variations due to the addition of LO only in the presence of phase inversion, i.e., for the 30/70 LDPE/PA6 blends containing a large amount of PA6. In the other cases, the variation extent is within the experimental error. The influence of LO and PA6 on the crystallographic parameters can be seen in the diffractograms reported in Figure 7. These show the

2Θ values of LDPE relative to the (110) and (200) planes: The values of 2Θ are in the sequence LDPE > LDPE/LO > LDPE/PA6/LO(50/50/4.17) > LDPE/PA6/LO(30/70/5.83). Therefore, there is an increasing shift of the diffraction angles, just confirming the synergistic effect of the PA6/LO pair already suggested by the data in Table VI.

CONCLUSIONS

In both binary LDPE/PA6 and ternary LDPE/PP/PA6 blends, LO and EV acted as compatibilizing agents, LO being the more effective one, as suggested by previous preliminary results.[41,42] In the case of binary blends, the compatibilization extent was found to depend not only on the amount of interfacial agents, but also on the LDPE/PA6 weight ratios.

The morphological analysis carried out on the blends, as they were and after their chemical etching,

Table XI   Interfacial Tensions Between LDPE and PA6 Without and With c.a.

System	$\gamma_{P1//P2}$ (dynes/cm)
LDPE//PA6	7.8
LDPE/LO//LO/PA6	0.1
LDPE/EV//EV/PA6	3.0

Table XII   Interfacial Tensions Between Polymers

	$\gamma_{P1//P2}$ (dynes/cm)
LDPE//PP	0.20
LDPE//PA6	7.83
PP//PA6	9.71
LDPE//LO	0.37
LDPE//EV	3.51
PP//LO	3.23
PP//EV	4.85
PA6//LO	5.19
PA6//EV	1.22

Table XIII   Degrees of Crystallinity (x), Apparent Crystal Sizes (D_{110}, in Å),
Cell Parameters (a, b, and c, in Å), and Specific Volumes (v in cm^3/g) of LDPE
in LDPE/PA6/LO Blends

LDPE/PA6/LO	x	$D_{110} \pm 5$	a	b	c	v
100/0/0	0.46	215	7.499	4.952	2.502	0.997
70/0/5	0.42	220	7.526	4.965	2.503	1.004
70/30/0	0.44	170	7.463	4.928	2.523	0.997
70/30/2.5[a]	0.39	180	7.582	4.981	2.541	1.030
70/30/5	0.41	180	7.575	4.980	2.531	1.025
70/30/10	0.39	175	7.629	4.998	2.529	1.035
50/50/0	0.43	160	7.501	4.934	2.512	0.998
50/50/4.17[a]	0.37	160	7.586	4.983	2.538	1.030
30/70/0	0.43	175	7.656	5.003	—	—
30/70/5.83[a]	0.33	145	7.658	4.998	—	—
0/0/100	n.d.	n.d.	7.614	5.001	2.520	1.031

[a] PA6/c.a. weight ratio = 30/2.5.

evidenced the dispersing power of LO and, to a lesser extent, of EV. DSC measurements on all the considered materials, chemical etchings, and elemental analysis of the PA6/c.a. systems stressed the occurring main PA6/c.a. interactions, especially when using LO. Also, mechanical tests confirmed LO to be more effective than is EV.

DSC measurements again, as well as WAXD determinations, showed that in LDPE/PA6/c.a. blends also LDPE/c.a. interactions occur and that these become stronger with the decrease of the LDPE/PA6 ratio, in opposition to what was observed for PA6/c.a. interactions. The compatibilization phenomenon and the different efficiency of the two interfacial agents were also justified by means of interfacial tension determinations.
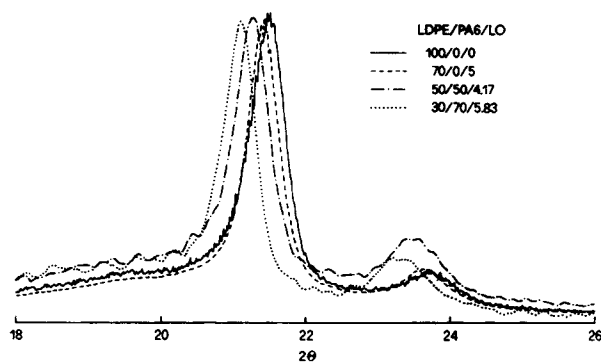

Figure 7   WAXD spectra of LDPE in different polymeric materials.

REFERENCES

1. A. J. Manson and L. H. Sperling, *Polymer Blends and Composites*, Haiden, New York, 1976.
2. D. R. Paul and S. Newman, *Polymer Blends*, Academic Press, New York, 1978.
3. G. Illing, in *Macromolecular Alloy Systems: A Contribution to the Determination of the Structure of Impact Resistant Polyamide-Polyolefin-Alloy, Polymer Blends: Processing Morphology and Properties*, E. Martuscelli, R. Palumbo, and M. Kryszewsky, Eds., Plenum, New York, 1980, p. 167.
4. O. Olablisi, L. M. Robertson, and T. H. Shaw, *Polymer-Polymer Miscibility*, Academic Press, New York, 1981.
5. J. Leidner, *Plastic Waste*, Marcel Dekker, New York, 1981.
6. L. A. Utraki, *Polym. Eng. Sci.*, **22**, 1166 (1982).
7. E. Martuscelli, in *First Mediterranean School on Science and Technology of Advanced Polymers-Based Materials*, Vico Equense, Italy, Sept. 11–22, 1989, p. 125.
8. D. Curto, A. Valenza, and F. P. La Mantia, *J. Appl. Polym. Sci.*, **39**, 865 (1990).
9. D. Acierno, A. Valenza, C. Dispenza, and G. Spadaro, in *European Symposium on Polymer Blends*, Capri (ITA), Maggio, 1993.
10. G. Spadaro, D. Acierno, E. Calderaro, and A. Valenza, *Radiat. Phys. Chem.*, **40**, 249 (1992).
11. D. Acierno and L. Di Maio, in *XI Convegno Italiano di Scienza e Tecnologia delle Macromolecule*, Torino, Sept. 1993.
12. P. L. Beltrame, A. Castelli, M. Canauz, M. Canetti, and A. Seves, *Makromol. Chem. Phys.*, **196**, 2715 (1995).
13. M. Arroyo and M. Lopez-Manchado, *Angew. Makromol. Chem.*, **226**, 129 (1995).

14. Y. Minoura, M. Ueda, S. Mizunuma, and M. Oba, *J. Appl. Polym. Sci.,* **13,** 1625 (1969).

15. R. L. Markham, *Adv. Polym. Tech.,* **10**(3), 231 (1990).

16. N. C. Liu and W. E. Baker, *Adv. Polym. Tech.,* **11**(4), 249 (1992).

17. L. Mascia and M. Xanthos, *Adv. Polym. Tech.,* **11**(4), 237 (1992).

18. S. Fuzessery, in *International Forum Davos Recycle '93,* Davos, Switzerland, March 22–26, 1993, 8/5-1.

19. P. Breant, in *International Forum Davos Recycle '93,* Davos, Switzerland, March 22–26, 1993, 8/4-1.

20. J. M. Willis, B. D. Favis, and C. Lavalée, *J. Mater. Sci.,* **28,** 1749 (1993).

21. J. M. Willis, V. Caldas, and B. D. Favis, *J. Mater. Sci.,* **26,** 4742 (1991), and references therein.

22. F. Ide and A. Hasegawa, *J. Appl. Polym. Sci.,* **18,** 963 (1974).

23. H. Raval, S. Devi, Y. P. Singh, and M. H. Mehta, *Polymer,* **32**(3), 493 (1991).

24. M. Canauz, A. Castelli, P. L. Beltrame, A. Siciliano, and A. Seves, in *6th International Conference on Polymer Supported Reactions in Organic Chemistry (POC 94),* Venice, June 19–23, 1994, Vol. 20, p. 4.

25. A. Castelli, M. Canauz, P. L. Beltrame, M. Canetti, and A. Seves, in *6th International Conference on Polymer Supported Reactions in Organic Chemistry (POC 94),* Venice, June 19–23, 1994, Vol. 20, p. 6.

26. B. Liang, J. L. White, J. E. Spruiell, and B. C. Goswami, *J. Appl. Polym. Sci.,* **28,** 2011 (1983).

27. M. J. Modic and L. A. Pottick, *Plast. Eng.,* **7,** 37 (1991).

28. H. Raval, S. Devi, Y. P. Singh, and M. H. Metha, *Polymer,* **32**(3), 493 (1991).

29. R. Holsti-Miettinen and J. Seppala, *Polym. Eng. Sci.,* **32**(13), 868 (1992).

30. M. Seadan, D. Graebling, and M. Lambia, *Polym. Net. Blends,* **3**(3), 115 (1993).

31. H. Moon, B. Ryoo, and J. Park, *J. Polym. Sci.,* **32,** 1427 (1994).

32. L. E. Alexander, *X-ray Diffraction Method in Polymer Science,* Wiley-Interscience, New York, 1969, p. 137.

33. S. Wu, *Polymer Interface and Adhesion,* Marcel Dekker, New York, Basel, 1982.

34. D. W. Van Krevelen, *Properties of Polymers,* 3rd ed., Elsevier, Amsterdam, 1992.

35. S. Wu, *J. Polym. Sci. Part C,* **34,** 19 (1971).

36. S. Wu, *J. Polym. Sci.,* **5,** 39 (1973).

37. S. Wu, *J. Colloid Interf. Sci.,* **31,** 153 (1969).

38. S. Wu, *J. Adhes.,* **5,** 39 (1973).

39. M. Langsam and G. J. Mantell, *J. Appl. Polym. Sci.,* **19,** 2235 (1975).

40. R. W. Phillips and R. H. Dettre, *J. Colloid Interf. Sci.,* **56,** 251 (1976).

41. A. Seves, A. Castelli, M. Di Pasquantonio, and P. L. Beltrame, *Mediterintec—First Mediterranean Exhibition of Technological Innovation,* Naples, Nov. 5–12, 1994.

42. M. Di Pasquantonio, *Thesis,* University of Milan, Italy, 1995.